Brazilian Journal
of Chemical
Engineering

ISSN 0104-6632
Printed in Brazil
www.abeq.org.br/bjche

Vol. 33, No. 02, pp. 373 - 382, April - June, 2016
dx.doi.org/10.1590/0104-6632.20160332s20140077

MATHEMATICAL MODELING OF BATCH ADSORPTION OF MANGANESE ONTO BONE CHAR

M. E. Maria and M. B. Mansur*

Departamento de Engenharia Metalúrgica e de Materiais, Universidade Federal de Minas Gerais,
Av. Antônio Carlos, 6627, Escola de Engenharia, Bloco 2, Sala 3634, Pampulha,
CEP: 31270-900, Belo Horizonte - MG, Brazil.
Phone: + (55) (31) 3409-1811, Fax: + (55) (31) 3409-1815
E-mail: marcelo.mansur@demet.ufmg.br

(Submitted: September 25, 2014 ; Revised: January 7, 2015 ; Accepted: March 20, 2015)

Abstract - The present study investigated the dynamics of batch adsorption of manganese onto bone char by using two distinct mathematical formulations: the diffusion model and the shrinking core model. Both models assumed spherical particles and adequately described the transient behavior of metal adsorption under changing operating conditions. Comparatively, the diffusion model described the manganese adsorption better at distinct particle sizes even when small particles were used ($d_p \leq 0.147$ mm); the shrinking core model proved to be more reliable when larger adsorbent particles were used ($d_p > 0.147$ mm), and it described experimental data better at changing solid-liquid ratios. Manganese adsorption was favored when: (i) smaller adsorbing particles were used due to the increase in the contact area and easier access to reacting sites of the char; however, such an effect proved to be limited to $d_p \leq 0.147$ mm, and (ii) higher solid-liquid ratios were used due to the increase in the available reacting sites. External and intraparticle mass transfer dependences on particle size and solid-liquid ratio were also investigated, and results corroborated with prior investigations found in the literature.
Keywords: Adsorption; Manganese; Bone char; Diffusion model; Shrinking core model.

INTRODUCTION

The treatment of industrial effluents containing dissolved metals is commonly done using chemical precipitation, which is a relatively simple operation and an efficient method to attend to legal requirements. The method, however, is not advantageous in the treatment of sulfuric aqueous solutions containing manganese, as is the case of acid rock drainage (ARD) effluents generated in the southeastern region of Brazil, because manganese presents high solubility within a wide range of pH (Bamforth *et al*., 2006). In fact, the precipitation of manganese may occur at high pH values of approximately 10-11. After the manganese has been removed, the pH of the effluent must be neutralized in order to discharge the treated water; therefore, the consumption of reagents is considerable. In addition, the quantity and the toxicity of the sludge will depend on the type and concentration of the dissolved metals. Therefore, it may result in a costly operation.

The removal and/or recovery of manganese from a typical nickel laterite waste solution was evaluated by Zhang *et al*. (2010) using distinct precipitation agents, such as hydroxides, carbonate, and SO_2/air oxidative mixture. The best result in terms of efficiency and economics was obtained by applying a combined method. Hydroxide or carbonate precipita-

*To whom correspondence should be addressed

tion was adequate for the removal/recovery of a large proportion of Mn(II), followed by oxidative precipitation applied to reduce manganese concentrations to a very low level. A literature review covering various separation and recovery methods, including solvent extraction, ion exchange, as well as hydroxide, carbonate, sulfide, and oxidative precipitations, is presented by Zhang and Cheng (2007). These methods are briefly compared and assessed in terms of their selectivity, efficiency, reagent costs, and product quality.

The adsorption of metals onto low cost sorbents, such as bone char, has also been evaluated as an alternative method to treat effluents (Choy and McKay, 2005; Giraldo and Moreno-Piraján, 2008; Kumar *et al*., 2010; Moreno *et al*., 2010; Martins *et al*., 2014; Vieira *et al*., 2014; Sicupira *et al*., 2014). Manganese, as well as cadmium, copper, iron, nickel and zinc, could be efficiently removed from sulfuric solutions at nearly neutral pH. As bone char consists basically of hydroxyapatite ($Ca_{10}(PO_4)_6(OH)_2$) and calcite ($CaCO_3$), it also raises the pH of the aqueous solution due to the dissolution of the calcite, thus contributing to a reduction in the lime consumed in the current treatment of ARD solutions containing manganese by means of chemical precipitation. In fact, the efficiency of metal adsorption is not favored in acidic medium due to proton competition at pH < 5.

Experimental results obtained by Moreno *et al*. (2010) and Sicupira *et al*. (2014) using ARD effluents revealed that manganese adsorption onto bone char followed satisfactorily the Langmuir equilibrium isotherm, with a value of q_m between 22 and 30 mg g^{-1}. This proved to be a chemisorption process, which is strongly influenced by operating variables, such as the pH of the aqueous phase and the solid/liquid ratio. Regarding its dynamics, manganese adsorption follows a pseudo-second order kinetic model (Ho, 2006). In addition, data fitting to simplified intraparticle diffusion models, such as those of Weber and Morris (1963), revealed that manganese diffusion within particles is the main rate-limiting step, whereas external mass transfer and intraparticle diffusion phenomena may also affect the removal of manganese when particles of smaller sizes are used.

In an attempt to evaluate the dynamics of manganese adsorption onto bone char and to identify the main phenomena that affect the process as a whole, two distinct models were developed in the present paper. In the diffusion model, the transient concentration of manganese is assessed by differential mass balances in the external aqueous phase and inside particles (Costodes *et al*., 2003). According to this model, both intraparticle and chemical reaction rates may occur simultaneously. Hence, metal concentration inside the particles depends on time and space. The diffusion model consists of a system of partial differential equations to be solved numerically. In the shrinking core model, two distinct regions (named reacted, or ash region, and non-reacted region) may exist inside particles, and the reaction front moves towards the center of the particle, while adsorption proceeds. In this case, metal concentration depends solely on time. The model consists of a system of ordinary differential equations whose numerical solution is much simpler to be obtained. However, the diffusion model is classical and it is normally applied to describe adsorption processes. In this context, the aim of the present work is evaluate how adequate the shrinking core model could describe manganese adsorption. A diffusion model was also developed for comparison purposes.

DEVELOPMENT OF BATCH ADSORPTION MODELS

To model the manganese adsorption onto bone char in a batch operation, the following assumptions were formulated: (i) the aqueous phase is an isothermal and incompressible fluid containing manganese at a known initial concentration and pH; (ii) the porous adsorbent particles of bone char are perfectly spherical, containing reacting sites that are homogeneously distributed within them; (iii) the reaction of manganese in the bone char particles is governed by a chemisorption mechanism (Sicupira *et al*., 2014); (iv) equilibrium is described by the Langmuir adsorption isotherm (Sicupira *et al*., 2014); (v) the system is perfectly mixed, so the external mass transfer process occurs solely in a thin boundary layer surrounding the particles, and (vi) the pH of the external phase is constant with time due to the buffer effect of calcite dissolution from the bone char.

Diffusion Model (DM)

The mass-balance equation of manganese in the bulk solution is given as follows:

$$-\frac{dC}{dt} = k_e A_S \left(C - C_i\big|_{r=R_p} \right) \tag{1}$$

The mass balance of manganese inside the spherical porous particles of bone char considers that: (i) mass transfer of metal is described mathematically by Fick's law, assuming an effective intraparticle diffusion coefficient that is constant and independent

of concentration, and (ii) the rate of adsorption of manganese is due to the chemical reaction that occurs at reacting sites that are homogeneously distributed within the particle (Crank, 1975).

$$\varepsilon \frac{\partial C_i}{\partial t} = \frac{D_{ef}}{r^2} \frac{\partial}{\partial r}\left(r^2 \frac{\partial C_i}{\partial r} \right) - \rho_a \frac{\partial q}{\partial t} \tag{2}$$

The equilibrium relation between q and C_i is given by the Langmuir adsorption isotherm (Sicupira *et al*., 2014):

$$q = \frac{a q_m C_i}{1 + a C_i} \tag{3}$$

The reaction by which the immobilized manganese is formed proceeds quite rapidly when compared with the diffusion process, and for this reason the kinetics are assumed to be instantaneous and not involved in the rate-controlling process (Teixeira *et al*., 2001; Lee and McKay, 2004; Jena *et al*., 2004); therefore, local equilibrium can be assumed to exist between the free $C_i(r,t)$ and immobilized $q(r,t)$ components of the diffusing manganese species. Hence, deriving Eq. (3) and substituting into Eq. (2):

$$\frac{\partial q}{\partial t} = \frac{\partial q}{\partial C_i}\frac{\partial C_i}{\partial t} = \frac{a q_m}{(1 + a C_i)^2}\frac{\partial C_i}{\partial t} \tag{4}$$

$$\left[\varepsilon + \frac{\rho_a a q_m}{\left(1 + a C_i\right)^2} \right] \frac{\partial C_i}{\partial t} = \frac{D_{ef}}{r^2} \frac{\partial}{\partial r}\left(r^2 \frac{\partial C_i}{\partial r} \right) \tag{5}$$

Equations (1) and (5) are subjected to the following initial and boundary conditions:

$$C(0) = C_0 \quad C_i(r,0) = 0 \tag{6}$$

$$\left.\frac{\partial C_i}{\partial r}\right|_{r=0} = 0 \tag{7}$$

$$-D_{ef} \left.\frac{\partial C_i}{\partial r}\right|_{r=R_p} = k_e \left(C - C_i\big|_{r=R_p} \right) \tag{8}$$

Shrinking Core Model (SCM)

According to this model, the adsorbing particle is surrounded by an external film and consists of two distinct regions schematically shown in Figure 1: the permeable product layer, which is loaded in manganese ($R_p \le r < r_c$), and the unreacted core, which shrinks uniformly as the reaction progresses ($r_c \le r \le 0$).

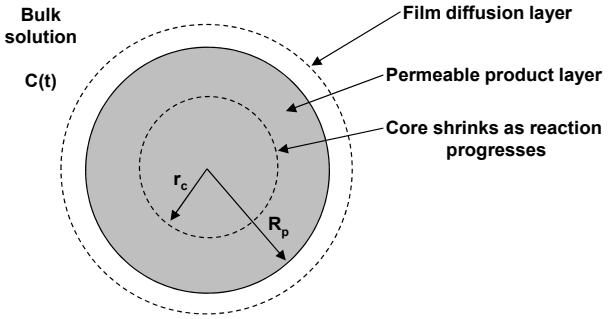

Figure 1: Spherical particle representation using the shrinking core model.

The reaction between Mn^{2+} ions and the reactant solid B of the char is assumed to be irreversible and occurs solely at the product-reactant interface ($r = r_c$) according to the following stoichiometric reaction:

$$Mn^{2+}_{(aq)} + b\ B_{(s)} \rightarrow Mn - B_{(immobilized)} \tag{9}$$

The model assumes that a pseudo steady-state approximation is valid and that the driving force in both external and particle mass transfer is linear, while the driving force in the reaction core incorporates the Langmuir isotherm. In the adsorbing particle, the relative effect of each resistance may change as the reaction proceeds because the length of the permeable product layer increases with time. If all mechanisms occur simultaneously, the system should be handled accordingly and the following rate expressions for each stage (film diffusion, product layer diffusion, and chemical reaction, respectively) can be formulated (Levenspiel, 1999; Han, 2002):

$$N(t) = 4\pi R_p^2 k_e \left(C - C_i\big|_{r=R_p} \right) =$$

$$= \frac{4\pi D_{ef} \left(C_i\big|_{r=R_p} - C_i\big|_{r=r_c} \right)}{\frac{1}{r_c} - \frac{1}{R_p}} = \tag{10}$$

$$= 4\pi r_c^2 k_r \left[C_i\big|_{r=r_c} - \frac{q}{a\left(q_m - q\right)} \right]$$

The adsorption rate $N(t)$ is related to the differential mass balance over the system by equating the decrease in manganese concentration in the solution with the accumulation of the adsorbate in the bone char and the mass balance on a spherical element of adsorbate particle as given by, respectively:

$$N(t) = -V\frac{dC}{dt} = W\frac{dq}{dt} = -\frac{4\pi r_c^2 \rho q_m}{b}\frac{dr_c}{dt} \tag{11}$$

Depending on which step of Equation (10) is slowest, that step is limiting for the overall adsorption process. Three limiting steps may occur: (i) diffusion through the film boundary layer (in this case, $C_i\big|_{r=R_p} = 0$), (ii) diffusion through the porous product layer (in this case, $C_i\big|_{r=R_p} = C$ and $C_i\big|_{r=r_c} = 0$), and (iii) chemical reaction at the reactant-product interface (in this case, $C_i\big|_{r=r_c} = C$). For each case, an equation giving the time required for a reaction to proceed from particle radius R_p to r_c can be obtained by integrating dr_c/dt with time from 0 to t (Han, 2002). If all mechanisms occur simultaneously, the mass-balance equation for manganese in the bulk solution is:

$$\frac{dC}{dt} = -\frac{\dfrac{4\pi R_p^2}{V}\left[C - \dfrac{q}{a\left(q_m - q\right)}\right]}{\dfrac{1}{k_e} + \dfrac{\left(R_p - r_c\right)R_p}{r_c D_{ef}} + \dfrac{R_p^2}{r_c^2 k_r}} \tag{12}$$

the average loading of manganese in the char is:

$$\frac{dq}{dt} = \frac{\dfrac{4\pi R_p^2}{W}\left[C - \dfrac{q}{a\left(q_m - q\right)}\right]}{\dfrac{1}{k_e} + \dfrac{\left(R_p - r_c\right)R_p}{r_c D_{ef}} + \dfrac{R_p^2}{r_c^2 k_r}} \tag{13}$$

and the temporal variation of the reacting-core radius is given by:

$$\frac{dr_c}{dt} = -\frac{\dfrac{bC}{\rho q_m}\left[C - \dfrac{q}{a\left(q_m - q\right)}\right]}{\dfrac{r_c^{\,2}}{R_p^2 k_e} + \dfrac{\left(R_p - r_c\right)r_c}{R_p D_{ef}} + \dfrac{1}{k_r}} \tag{14}$$

Equations (12)-(14) were subjected to the following initial conditions:

$$C(0) = C_0 \qquad q = 0 \qquad r_c(0) = R_p \tag{15}$$

According to this model, the adsorption rate of manganese onto bone char is controlled by the respective resistances to film diffusion, product layer diffusion, and chemical reaction. If an instantaneous reaction within spherical adsorbent particles prevails, the third resistance of Eqs. (12)-(14) is null.

Numerical Solution of Models and Estimation of Parameters

Both models were solved numerically using MATLAB software (Version 7.0). The diffusion model, Eqs. (1), (5)-(8), contains a partial differential equation, which was discretized using the implicit finite difference method. Other numerical methods, such as Crank-Nicholson's implicit finite difference method; a semi-analytical solution method; and the Cartesian collocation method were compared elsewhere in terms of accuracy, stability, convergence, and computation in CPU time (Lee and McKay, 2004; McKay, 2001). The solution of the shrinking core model, Eqs. (12)-(15), was obtained using the fourth-order Runge-Kutta method. The same numerical solution was used by Sarkar and Bandyopadhyay (2011) and Jena *et al*. (2004). Properties such as accuracy, stability, convergence and computational time of the numerical methods used in the present work are available elsewhere (Hoffman, 1992; Pinto and Lage, 2001).

Experimental data obtained by Sicupira *et al*. (2014) using laboratory solutions containing manganese were fitted to both models in an attempt to assess the values of mass transfer and chemical reaction rate parameters under changing operating conditions. The estimation of parameters was done numerically by minimizing an objective function (F) using an optimization routine found in MATLAB software based on the Nelder-Mead simplex direct search method (Lagarias *et al*., 1998). The objective function adopted in this work is the sum of the squared deviation between estimated (C_{est}) and experimental (C_{exp}) concentrations of manganese in the external aqueous phase:

$$F = \sum_{j=1}^{N_{\exp}} \left(C_{est,j} - C_{\exp,j}\right)^2 \tag{16}$$

The relative error in terms of percentage was calculated to measure how close estimated concentrations are to the experimental concentrations:

$$\text{relative error} = \frac{100}{N_{\text{exp}}} \sum_{j=1}^{N_{\text{exp}}} \frac{\left| C_{est,j} - C_{\text{exp},j} \right|}{C_{\text{exp},j}} \qquad (17)$$

RESULTS AND DISCUSSION

Physical consistency of the shrinking core model was evaluated by simulating the individual effects of film diffusion, product layer diffusion and chemical reaction resistances. Calculations were done by changing the magnitude of the external mass transfer coefficient (k_e), the intraparticle effective diffusion coefficient (D_{ef}), and the reaction rate constant (k_r). The simulations shown in Figure 2 were performed according to the operating conditions portrayed in Table 1. Typical transient concentration profiles in the external aqueous phase were reproduced, i.e., manganese concentration diminished with time until it reached a condition of equilibrium, depending on the operating conditions.

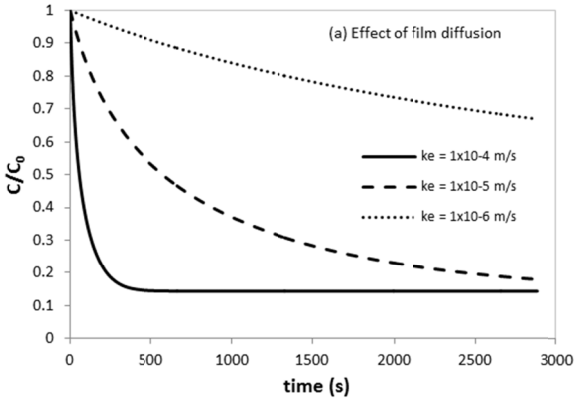

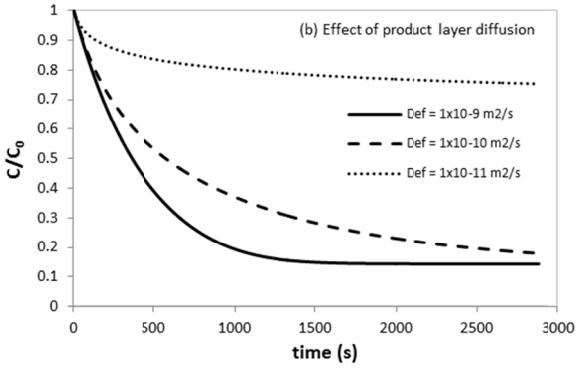

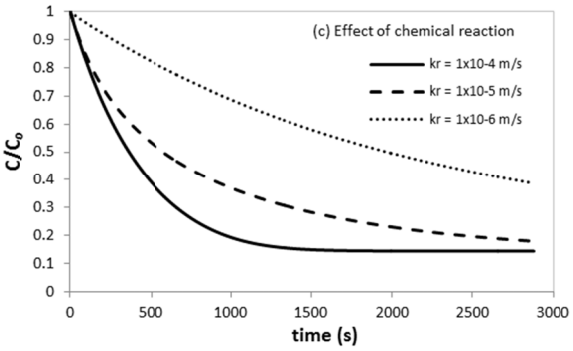

Figure 2: Sensitivity analysis of the shrinking core model: (a) Film diffusion resistance ($D_{ef} = 10^{-10}$ m^2 s^{-1} and $k_r = 10^{-5}$ m s^{-1}), (b) Product layer diffusion resistance ($k_e = 10^{-5}$ m s^{-1} and $k_r = 10^{-5}$ m s^{-1}), and (c) Chemical reaction resistance ($k_e = 10^{-5}$ m s^{-1} and $D_{ef} = 10^{-10}$ m^2 s^{-1}) (S/L = 2/400 g mL^{-1}; d_p = 0.833 mm; C_0 = 100 mg L^{-1}; pH$_i$ = 5.76).

Table 1: Operating conditions of simulated batch adsorption of manganese onto bone char (Sicupira *et al.*, 2014).

Parameter	Symbol	Unity	Value
Initial concentration of manganese in the external phase	C_0	mg L^{-1}	100
Volume of aqueous phase	V	L	0.4
Surface area of bone char	a_p	m^2 g^{-1}	93
Stoichiometric constant	b	-	1
Particle porosity	ε	-	0.7975
Real density of particle	ρ	g cm^{-3}	2.9

Intraparticle resistance normally governs the adsorption processes; however, the effect of the external mass transfer resistance is significant for the conditions simulated herein, mainly when $k_e < 10^{-5}$ m s^{-1}, as shown in Figure 2(a). External mass transfer rates from or to solid particles suspended in an agitated liquid are affected by a number of variables, such as particle diameter, viscosity of the liquid, type of impeller, clearance, agitation speed, vessel geometry, etc. The smaller the value of k_e, the higher the external resistance for manganese to reach the adsorbent particles; consequently, a lower adsorption rate is obtained. Jadhav and Pangarkar (1991) presented a survey of the literature, including various correlations and the observed effects of typical variables on such mass transfer coefficients. The intraparticle mass transfer resistance also increases when the value of D_{ef} decreases, slowing down the manganese diffusion as shown in Figure 2(b). And finally, the effect of chemical reaction shown in Figure 2(c) reveals that faster kinetics favor manganese adsorption. This effect, however, is much less pronounced than those observed for mass transfer effects in the

simulated conditions. As evidenced by Crank (1975), the effect of instantaneous reaction is to slow down the diffusion process.

The effect of particle size on the batch adsorption of manganese onto bone char is shown in Figure 3, including simulations using the diffusion model (DM) and the shrinking core model (SCM). Determination coefficients and relative errors for both models are displayed in Table 2. Decreasing the particle size resulted in a shorter time to reach equilibrium. The kinetics is quite rapid at the beginning of the process, mainly if smaller particles are used, which is related to a larger contact area and easier contact with reacting sites of the char, and slows down over time until it reaches equilibrium. The particle size affects the adsorption kinetics at shorter times, but it has little effect at longer times. According to the transient behavior shown in Figure 3, however, such effects are limited when particles with $d_p \leq 0.147$ mm were used.

Table 2: Fitting parameters of the diffusion and shrinking core models for different particle sizes (S/L = 2/400 g mL^{-1}; C_0 = 100 mg L^{-1}; pH$_i$ = 5.76).

Diameter of particle (mm)	Diffusion model		Shrinking core model	
	Determination coefficient (R^2)	Relative error (%)	Determination coefficient (R^2)	Relative error (%)
< 0.053	0.9701	14.2	0.9667	18.3
0.104-0.147	0.9719	13.7	0.9626	19.7
0.417-0.833	0.9731	13.9	0.9972	2.9

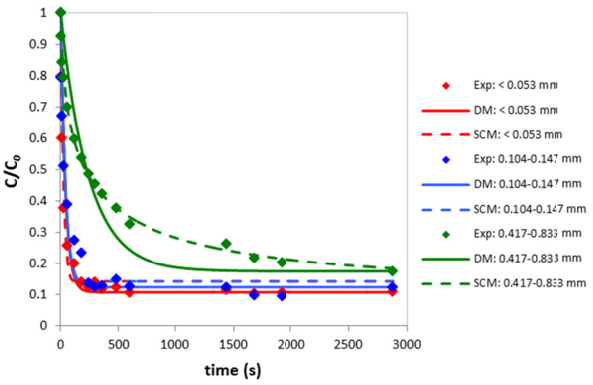

Figure 3: Effect of particle size on the adsorption of manganese onto bone char (S/L = 2/400 g mL^{-1}; C_0 = 100 mg L^{-1}; pH$_i$ = 5.76).

By comparing the simulations from both models, it can be seen that the diffusion model described the experimental transient behavior quite well ($R^2 > 0.97$ and relative error < 15%), even when smaller particle diameters were used ($d_p \leq 0.147$ mm). In these conditions, a sharp decrease in the concentration of manganese occurred at shorter times, stabilizing afterwards. The shrinking core model also described such behavior satisfactorily ($R^2 > 0.96$ and relative error < 20%). However, fitting was comparatively poorer than that obtained by the diffusion model when small particles were used, most likely because the unreacted and reacted regions might not be very well defined in smaller dimensions. Therefore, the shrinking core model proved to be more reliable when larger particles of the adsorbent were used ($d_p \geq 0.417$ mm, with $R^2 > 0.99$ and relative error < 3%).

Regarding the effect of solid-liquid ratio, the results portrayed in Figure 4 reveal that a higher percentage of manganese removal was obtained with the increase in the solid-liquid ratio due to the increase in the quantity of reacting char. As expected, a longer time was required to load the adsorbent with the increase in the solid-liquid ratio, despite the faster kinetics of manganese adsorption identified at times of first contact. In these simulations, the shrinking core model described data comparatively better ($R^2 > 0.99$ and relative error < 10%) than the diffusion model ($R^2 > 0.95$ and relative error < 35%), probably because larger particles of the adsorbent were used in these runs (Table 3).

Table 3: Fitting parameters of the diffusion and shrinking core models for different solid-liquid ratios (d_p = 0.417-0.833 mm; C_0 = 100 mg L^{-1}; pH$_i$ = 5.76).

Solid-liquid ratio (g mL^{-1})	Diffusion model		Shrinking core model	
	Determination coefficient (R^2)	Relative error (%)	Determination coefficient (R^2)	Relative error (%)
1/400	0.9833	2.8	0.9907	1.8
2/400	0.9731	13.9	0.9972	2.9
3/400	0.9597	32.8	0.9967	8.4

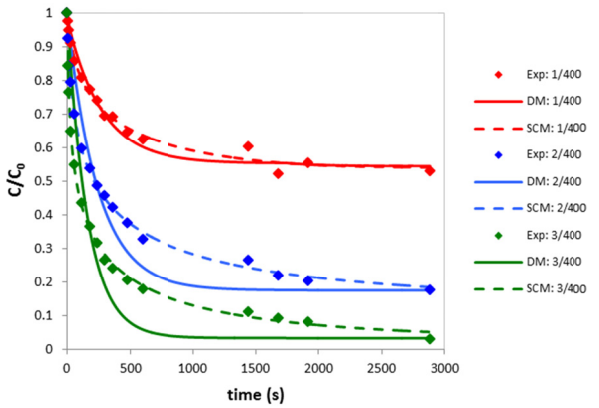

Figure 4: Effect of solid-liquid ratio on the adsorption of manganese onto bone char (d_p = 0.417-0.833 mm; C_0 = 100 mg L^{-1}; pH$_i$ = 5.76).

The transport coefficients k_e and D_{ef} assessed by data fitting using both models assuming instantaneous reaction to describe the batch adsorption of manganese onto bone char in the operating conditions investigated by Sicupira *et al*. (2014) are displayed in Figure 5. The effect of correlation between fitted parameters was not pronounced, since, for each operating condition, the solution practically converged to the same result with different initial guesses of parameters. Power law equations were chosen to correlate data of the transport coefficients as a function of the investigated operating conditions. Although in some cases the R^2-values were poor, such equations are commonly used to describe self-similar systems (no preferred length scale), as verified in ramified structures such as fractals and adsorbent particles (Do and Nguyen, 1988). As previously shown, the diffusion model described the effect of particle size better, while the shrinking core model described the effect of the solid-liquid ratio better. Nevertheless, the estimates obtained by using both models were included in Figure 5 for comparison purposes; the model with a higher determination coefficient (R^2) is represented by a wide continuous curve, while the other is represented by a narrow dashed curve.

The average dependence of k_e on $d_p^{-0.5}$ was practically obtained for both models, as shown in Figure 5(a). Such a result corroborates a number of previous investigations (Harriot, 1962; Kuboi *et al*., 1974; Asai *et al*., 1988; Armenante and Kirwan, 1989; Jadhav and Pangarkar, 1991). Values of the external mass transfer coefficients of manganese to or from a sphere to an infinite stagnant fluid, which yields $Sh = 2$ (Sherwood number is given by $Sh = k_e d_p / D_{Mn,water}$, with molecular diffusivity of manganese in water $D_{Mn,water} = 6.88\text{x}10^{-10}$ m^2 s^{-1} at 25 °C, according to Domenico and Schwartz, 1998) is also shown in Figure 5(a). The positive deviation from this limiting value is attributed to the convective contribution. Relatively higher deviations between estimates from both models were observed when small particles were used ($d_p \leq 0.147$ mm), thus evidencing the significant decrease in the external mass transfer resistance of manganese when microparticles are used as adsorbents. Concerning the effect of the solid-liquid ratio on the external mass transfer coefficient shown in Figure 5(b), it was found to be of little importance, with an average value of $k_e = (13\pm4)\text{x}10^{-6}$ m s^{-1} when considering estimates from both models, thus corroborating the experimental findings of Asai *et al*. (1988).

An opposite behavior with dependence $D_{ef} \propto d_p^{0.6}$ was identified by data fitting using the diffusion model (Figure 5(c)). External and internal mass transfer resistances are closely connected according to the boundary condition, Eq. (8), so a higher intraparticle resistance was expected. In addition, a longer diffusion path is expected when bigger adsorbent particles are used. Therefore, the results obtained may be attributed to diffusion in pores of different class sizes. As regards the effect of the solid-liquid ratio on the intraparticle diffusion coefficient shown in Figure 5(d), a significant increase in the internal resistance was found when higher solid-liquid ratios were used (dependence $D_{ef} \propto (S/L)^{-1.5}$), which is due to the increase in the amount of porous particles.

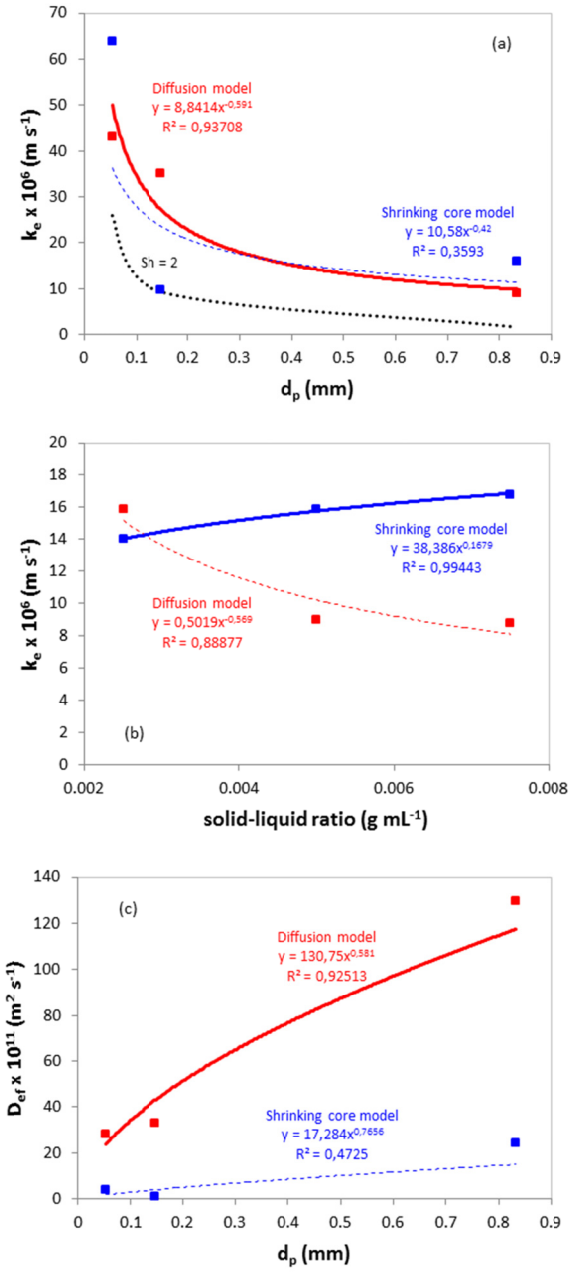

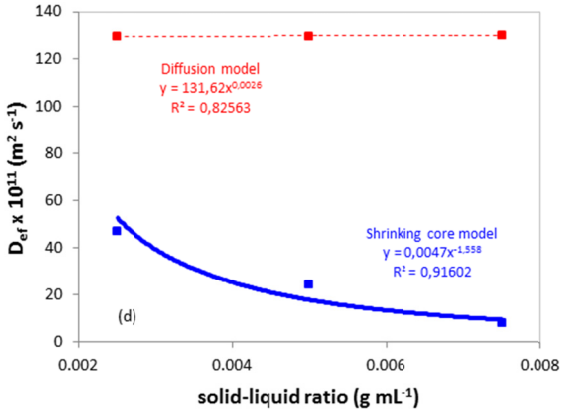

Figure 5: Transport coefficients k_e and D_{ef} assessed by data fitting with the diffusion model and shrinking core model assuming instantaneous reaction under the operating conditions investigated by Sicupira *et al*. (2014).

The Biot number for mass transfer (which is analogous to the Biot number for transient heat transfer) is defined as the ratio of external to internal mass transfer resistances ($Bi_m = k_e d_p / D_{ef}$). If $Bi_m > 0.1$, mass transfer resistance within particles is significant (Incropera *et al*., 2007). According to such a parameter, pore diffusion was found to predominate for all operating conditions investigated by Sicupira *et al*. (2014). Therefore, the manganese concentration profile is not uniform throughout the adsorbent particles.

CONCLUSIONS

The batch adsorption of manganese onto bone char was modeled using two mathematical approaches assuming spherical particles: the diffusion model and the shrinking core model. Simulations were compared with experimental data and the following conclusions were drawn:

- Both models adequately described the transient behavior of metal adsorption. In fact, manganese concentration in the external aqueous phase diminished monotonically over time until it reached equilibrium, which depended on the given operating conditions;
- The diffusion model described the effect of particle size better, while the shrinking core model described the effect of the solid-liquid ratio better. Manganese adsorption was favored when: (i) smaller adsorbing particles were used due to the increase in the contact area and easier access to reacting sites of the char, but such an effect was found to be limited to $d_p \leq 0.147$ mm, and (ii) higher solid-liquid ratios were used due to the increase in the available reacting sites;
- External and intraparticle mass transfer coefficients were evaluated for changing particle sizes and solid-liquid ratios. Dependences assessed in the present work corroborated prior studies found in the literature. Intraparticle mass transfer was found to dominate the adsorption of manganese onto bone char under the operating conditions investigated.

ACKNOWLEDGMENTS

The authors wish to acknowledge PPGEM/UFMG and the Brazilian agencies FAPEMIG (TEC-APQ-04026-10), CNPq (304788/2012-0), CAPES-PROEX, and INCT Acqua (www.acqua-inct.org) for their financial support.

NOMENCLATURE

a	affinity parameter of Langmuir isotherm (L mg^{-1})
a_p	surface area of bone char particles (m^2 g^{-1})
A_S	superficial area of adsorbent particles (m^2 m^{-3})
b	stoichiometric constant defined by Eq. (9) (-)
B	reactant solid defined by Eq. (9) (-)
Bi_m	Biot number of mass transfer (-)
C	concentration of manganese in the bulk external phase (mg L^{-1})
C_0	initial concentration of manganese in the external bulk phase (mg L^{-1})
C_i	concentration of manganese within the adsorbent particle (mg L^{-1})
D_{ef}	effective diffusion coefficient (m^2 s^{-1})
d_p	diameter of adsorbent particle (m)
F	objective function defined by Eq. (16) (-)
k_e	mass transfer coefficient in the bulk external phase (m s^{-1})
k_r	reaction rate constant for heterogeneous systems (m s^{-1})
$N(t)$	adsorption rate at time t (mg s^{-1})
q	concentration of immobilized manganese within the adsorbent particle (mg g^{-1})
q_m	theoretical maximum adsorption capacity of Langmuir isotherm (mg g^{-1})
r	radial distance from the center of the particle, $0 < r < R_p$ (m)
R_p	radius of adsorbent particle (m)
R^2	determination coefficient (-)
r_c	unreacted core radius (m)

Sh	Sherwood number (-)
S/L	solid-liquid ratio (g mL^{-1})
t	time (s)
V	volume of aqueous phase (L)
W	weight of the adsorbent (g)

Greek Symbols

ε	particle porosity (-)
ρ	density of adsorbent particle (g m^{-3})
ρ_a	apparent density of adsorbent particle (g m^{-3})

REFERENCES

Armenante, P. M., Kirwan, D. J., Mass transfer to microparticles in agitated systems. Chemical Engineering Science, 44, 2781-2796 (1989).

Asai, S., Konishi, Y., Sasaki, Y., Mass transfer between fine particles and liquids in agitated vessels. Journal of Chemical Engineering of Japan, 21, 107-112 (1988).

Bamforth, S. M., Manning, D. A. C., Singleton, I., Younger, P. L., Johnson, K. L., Manganese removal from mine waters - investigating the occurrence and importance of manganese carbonates. Applied Geochemistry, 21, 1274-1287 (2006).

Choy, K. K. H., McKay, G., Sorption of metal ions from aqueous solution using bone char. Environment International, 31, 845-854 (2005).

Costodes, T., Fauduet, V. C., Porte, H., Delacroix, C. A., Removal of Cd(II) and Pb(II) ions, from aqueous solutions, by adsorption onto sawdust of *Pinus sylvestris*. Journal of Hazardous Materials, 105, 121-142 (2003).

Crank, J., The Mathematics of Diffusion. 2nd Ed., Clarendon Press, Oxford (1975).

Do, D. D., Nguyen, T. S., A power law adsorption model and its significance. Chemical Engineering Communications, 72, 171-185 (1988).

Domenico, P. A., Schwartz, F. W., Physical and Chemical Hydrogeology. 2nd ed., John Wiley & Sons, USA (1998).

Giraldo, L., Moreno-Piraján, J. C., Pb^{2+} adsorption from aqueous solutions on activated carbons obtained from lignocellulosic residues. Brazilian Journal of Chemical Engineering, 25(1), 143-151 (2008).

Han, K. N., Fundamentals of aqueous metallurgy. SME, USA (2002).

Harriott, P., Mass transfer to particles – Part I: Suspended in agitated vessels. AIChE Journal, 8, 93-102 (1962).

Ho, Y. S., Review of second-order models for adsorption systems. Journal of Hazardous Materials, B136, 681-689 (2006).

Hoffman, J. D., Numerical Methods for Engineers and Scientists. McGraw-Hill, New York, USA (1992).

Incropera, F. P., Dewitt, D. P., Bergman, T. L., Lavine, A. S., Fundamentals of Heat and Mass Transfer. 6th Ed., John Wiley & Sons, USA (2007).

Jadhav, S. V., Pangarkar, V. G., Particle-liquid mass transfer in mechanically agitated contactors. Industrial & Engineering Chemistry Research, 30, 2496-2503 (1991).

Jena, P. R., Basu, J. K., De, S., A generalized shrinking core model for multicomponent batch adsorption process. Chemical Engineering Journal, 102, 267-275 (2004).

Kuboi, R., Komasawa, I., Otake, T., Iwasa, M., Fluid and particle motion in turbulent dispersion – III: Particle liquid hydrodynamics and mass transfer in turbulent dispersion. Chemical Engineering Science, 29, 659-668 (1974).

Kumar, P. S., Ramakrishnan, K., Kirupha, S. D., Sivanesan, S., Thermodynamic and kinetic studies of cadmium adsorption from aqueous solution onto rice husk. Brazilian Journal of Chemical Engineering, 27(2), 347-355 (2010).

Lagarias, J. C., Reeds, J. A., Wright, M. H., Wright, P. E., Convergence properties of the Nelder-Mead simplex method in low dimensions. SIAM Journal Optimization, 9, 112-147 (1998).

Lee, V. K. C., McKay, G., Comparison of solutions for the homogeneous surface diffusion model applied to adsorption systems. Chemical Engineering Journal, 98, 255-264 (2004).

Levenspiel, O., Chemical Reaction Engineering. 3rd Ed., John Wiley & Sons, USA (1999).

Martins, R. J. E., Vilar, V. J. P., Boaventura, R. A. R., Kinetic modeling of cadmium and lead removal by aquatic mosses. Brazilian Journal of Chemical Engineering, 31(1), 229-242 (2014).

McKay, G., Solution to the homogeneous surface diffusion model for batch adsorption systems using orthogonal collocation. Chemical Engineering Journal, 81, 213-221 (2001).

Moreno, J. C., Gómez, R., Giraldo, L., Removal of Mn, Fe, Ni and Cu ions from wasterwater using cow bone charcoal. Materials, 3, 452-466 (2010).

Pinto, J. C., Lage, P. L. C., Métodos numéricos em problemas de engenharia química. E-papers, Rio de Janeiro, Brazil (2001). (In Portuguese).

Sarkar, D., Bandyopadhyay, A., Shrinking core model in characterizing aqueous phase dye adsorption. Chemical Engineering Research & Design, 89,

69-77 (2011).
Sicupira, D. C., Silva, T. T., Leão, V. A., Mansur, M. B., Batch removal of manganese from acid mine drainage using bone char. Brazilian Journal of Chemical Engineering, 31, 195-204 (2014).
Teixeira, V. G., Coutinho, F. M. B., Gomes, A. S., The most important methods for the characterization of porosity of styrene-divinylbenzene based resins. Química Nova, 24, 808-818 (2001). (In Portuguese).
Vieira, M. G. A., de Almeida Neto, A. F., da Silva, M. G. C., Carneiro, C. N., Melo Filho, A. A., Adsorption of lead and copper ions from aqueous effluents on rice husk ash in a dynamic system. Brazilian Journal of Chemical Engineering, 31(2), 519-529 (2014).
Weber, W. J., Morris, J. C., Kinetic of adsorption carbon solution. Journal of Sanitary Engineering Divisor, American Society Civil Engineers, 89, 31-59 (1963).
Zhang, W., Cheng, C. Y., Manganese metallurgy review. Part II: Manganese separation and recovery from solution. Hydrometallurgy, 89, 160-177 (2007).
Zhang, W., Cheng, C. Y., Pranolo, Y., Investigation of methods for removal and recovery of manganese in hydrometallurgical processes. Hydrometallurgy, 101, 58-63 (2010).